Vibrated granular bed on a bumpy surface

Eldin Wee Chuan Lim*
Department of Chemical and Biomolecular Engineering, National University of Singapore, 4 Engineering Drive 4, Singapore 117576, Singapore

(Received 1 September 2008; revised manuscript received 1 February 2009; published 9 April 2009)

We investigate effects of physical characteristics of the vibrating base in a vibrated granular bed system on the bulk granular behavior of the bed using molecular dynamics simulations. With a vibrating base that exhibits low coefficient of restitution for particle-base collisions, a monolayer of granular materials was observed to form dynamically on the surface of the base. Such a system was shown to be both qualitatively and quantitatively equivalent to one with a bumpy base composed of discrete solid particles undergoing the same type of imposed oscillatory motion. The "bumpiness" of such a base, as defined by the size of particles constituting the vibrating base, was also found to have insignificant effects on the behavior of the bulk granular materials. The observations made in this study may point toward a possible methodology to model vibrating granular bed systems with inelastic bases using continuum theories.

DOI: 10.1103/PhysRevE.79.041302 PACS number(s): 81.05.Rm, 83.10.Rs, 83.80.Fg

I. INTRODUCTION

A bed of granular materials subjected to vertical vibrations exhibits a variety of interesting phenomena and has been the focus of many research studies in recent years. It represents a good scientific model for various important industrial applications involving granular solid processing such as mixers, dryers, and shakers. More fundamentally, a vibrated granular bed is also an example of a highly nonlinear dynamical system which exhibits pattern formation and hydrodynamic instabilities. Research in this area has, in general, proceeded via two approaches, experimental and computational. Pak and Behringer [1] carried out experiments on vertically vibrated sand confined within an annular space and observed a type of surface wave motion unique to granular materials with a relatively large dynamic angle of repose. Melo *et al.* [2] reported on the formation of square and stripe patterns in vertically oscillated layers of glass beads in a cylindrical container. The wavelength of the pattern was found to be independent of layer depth but obeyed an inverse square law with respect to vibrating frequency. Transitions between the patterns could be achieved by varying the vibrating frequency at constant dimensionless acceleration. With varying dimensionless acceleration, other standing-wave patterns, such as hexagons and kinks, were observed [3]. Umbanhowar *et al.* [4] observed the formation of stable two-dimensional localized excitations, which they termed oscillons, in a vibrated layer of sand. Tsimring and Aranson [5] proposed a phenomenological model to describe pattern formation in vibrated granular materials and showed that conservation of mass played a significant role in the pattern formation phenomenon. Stable cellular patterns such as standing rolls and squares, oscillons, and worms could be simulated by the model.

With the advent of computational power in recent years, computer simulations have become a useful complement to experimental studies in elucidating some of the subtle aspects of granular behavior. The method of molecular dynamics, in particular, has been established to be capable of reproducing computationally the various types of patterns observed in such granular systems. Aoki and Akiyama [6] conducted a two-dimensional simulation and observed surface wave pattern formation corresponding to that seen in an experimental setup. The simulation revealed that shear dissipation forces played an important role in the formation of such patterns. Subsequently, Bizon *et al.* [7] carried out three-dimensional simulations using an event-driven algorithm and corresponding experimental studies using lead spheres. They reported remarkably similar standing-wave patterns obtained from the two approaches under various operating conditions, validating the usefulness of the modeling approach for examining details of such granular systems which may be difficult to measure experimentally.

Various aspects of the vibrated granular bed system, such as effects of the dimensionless acceleration imposed on the vibrating base, amount, type, and size distribution of the granular materials on the collective behavior and pattern formation phenomenon of the bed, have been investigated fairly extensively in the research literature. Others, in contrast, have remained conspicuously unexplored so far. One such aspect relates to the nature of the base on which granular materials in a vibrated bed system is oscillated. In computational studies, the vibrating base is usually assumed, for sake of simplicity, to be perfectly flat and to have a coefficient of restitution close to unity for particle-base collisions. The implication of this assumption toward realistic modeling of such vibrated granular bed systems forms the basis of the present study. Deng and Wang [8] have presented photographs of the cross section of a vibrated granular bed taken using a charge-coupled device camera (see Fig. 2 of [8]). It may be discerned that, on close inspection of their figure, there exists a fairly thin layer of granular materials adhered to the vibrating base during its downward motion. In contrast, typical snapshots obtained from computer simulations which apply the molecular-dynamics type of modeling approach usually show a "clean" base devoid of any solid particles [6,9]. The system of Deng and Wang [8] consisted of

*Corresponding author; FAX: (65) 6779 1936; chelwce@nus.edu.sg

glass beads vibrated in a square-base vessel made of Perspex. The particle-base coefficient of restitution was not reported but we postulate here based on empirical observation that it might have been fairly low. Although other factors, such as the accumulation of electrostatic charges leading to generation of strong adhesive forces between particles and base, might have been present and been equally important, they will not be considered within the scope of this paper. As will be shown later, we confirm through molecular-dynamics type simulations that a low particle-base coefficient of restitution will indeed result in a thin granular layer adhering to the vibrating base. We show further that this is qualitatively and quantitatively equivalent to a vibrated granular bed system with a bumpy vibrating base. Finally, we explore effects of this "bumpiness" of the base on the collective behaviors of granular materials within the system.

II. MODEL

The molecular-dynamics approach to modeling of granular systems, otherwise known as the discrete element method (DEM), has been applied extensively for studies of various aspects of granular behavior. Some examples of such studies, as seen from recent publications, include studies of packing of particles under controlled mechanical vibrations [10], density wave and coherent structure formation in a Couette geometry [11], and flow behaviors in various types of multiphase systems [12–16]. For a comprehensive review on this topic, the interested reader is referred to a recent review paper by Zhu *et al.* [17]. The methodology of DEM and its corresponding governing equations have also been presented numerous times in the research literature (see, e.g., [18]) and only a brief description will be presented here for sake of completeness.

The translational and rotational motions of individual solid particles are governed by Newton's laws of motion:

$$m_i \frac{dv_i}{dt} = \sum_{j=1}^{N} (f_{c,ij} + f_{d,ij}) + m_i g, \tag{1}$$

$$I_i \frac{d\omega_i}{dt} = \sum_{j=1}^{N} T_{ij}, \tag{2}$$

where m_i and v_i are the mass and velocity of the ith particle, respectively, N is the number of particles in contact with the ith particle, $f_{c,ij}$ and $f_{d,ij}$ are the contact and viscous contact damping forces, respectively, I_i is the moment of inertia of the ith particle, ω_i is its angular velocity, and T_{ij} is the torque arising from contact forces which causes the particle to rotate.

Contact and damping forces have to be calculated using force-displacement models that relate such forces to the relative positions, velocities, and angular velocities of the colliding particles. Following Lim [18], a linear spring-and-dashpot model is implemented for the calculation of these collision forces. With such a closure, interparticle collisions are modeled as compressions of a perfectly elastic spring while the inelasticities associated with such collisions are modeled by the damping of energy in the dashpot component of the model. Collisions between particles and a wall may be handled in a similar manner but with the latter not incurring any change in its momentum. In other words, a wall at the point of contact with a particle may be treated as another particle but with an infinite amount of inertia. The normal ($f_{cn,ij}$, $f_{dn,ij}$) and tangential ($f_{ct,ij}$, $f_{dt,ij}$) components of the contact and damping forces are calculated according to the following equations:

$$f_{cn,ij} = -(\kappa_{n,i}\delta_{n,ij})n_i, \tag{3}$$

$$f_{ct,ij} = -(\kappa_{t,i}\delta_{t,ij})t_i, \tag{4}$$

$$f_{dn,ij} = -\eta_{n,i}(v_r n_i)n_i, \tag{5}$$

$$f_{dt,ij} = -\eta_{t,i}\{(v_r t_i)t_i + (\omega_i \times R_i - \omega_j \times R_j)\}, \tag{6}$$

where $\kappa_{n,i}$, $\delta_{n,ij}$, n_i, and $\eta_{n,i}$, and $\kappa_{t,i}$, $\delta_{t,ij}$, t_i, and $\eta_{t,i}$ are the spring constants, displacements between particles, unit vectors, and viscous contact damping coefficients in the normal and tangential directions, respectively, v_r is the relative velocity between particles, and R_i and R_j are the radii of particles i and j, respectively. If $|f_{ct,ij}| > |f_{cn,ij}|\tan\phi$, then "slippage" between two contacting surfaces is simulated based on Coulomb-type friction law, i.e., $|f_{ct,ij}| > |f_{cn,ij}|\tan\phi$, where $\tan\phi$ is analogous to the coefficient of friction.

We focus our attention next on the vibrated granular bed system of interest to the present work, namely, that used by Deng and Wang [8] in their recent experimental studies. It may be easily estimated from the total mass of granular materials used by these authors in their system that the total number of solid particles (0.5 mm glass beads) was on the order of 10^9, which by present day standards, is prohibitively large for computational modeling using the DEM approach. We therefore consider a two-dimensional vertical cross section of the system (140 mm width $\times$ 140 mm height) of one-particle thickness in the spanwise direction. Two vertical walls are imposed on each end of the system in the horizontal direction so as to correspond as closely as possible to the actual physical system used by the previous researchers. Under random packing conditions and with the entire system at rest, this pseudo-three-dimensional control volume is estimated to contain a reasonable 4000 glass beads, amounting to about 14 layers of granular materials. The base of the system is simulated to undergo a sinusoidal motion such that its displacement from the equilibrium position is described by $A\sin(\omega t)$, where A is the amplitude of the oscillatory motion, $\omega = 2\pi f$ is the angular frequency, and t is time. To simulate a vibrated granular bed system with fairly elastic particle-particle collisions and moderately inelastic particle-base collisions so as to test the postulate made earlier, values of coefficient of restitution $\varepsilon_p = 0.86$ and $\varepsilon_b = 0.46$ were used for the two types of collisions, respectively. Other pertinent simulation parameters are presented in Table I. In the first part of the present study, the vibrating frequency and amplitude were varied in the range of 8–32 Hz and 1.09–17.48 mm, respectively, to cover a reasonable range of values of the dimensionless acceleration, $\Gamma = \frac{4\pi^2 f^2 A}{g}$. As will be explained later, the entire set of simulation was then repeated

TABLE I. Material properties and system parameters.

Shape of particles	Spherical
Number of particles	4000
Particle diameter, d	0.5 mm
Particle density, ρ_p	2500 kg m^{-3}
Coefficient of restitution, ε_p	0.86
Coefficient of restitution, ε_b	0.46
Coefficient of friction	0.3
System dimensions	140 mm width $\times$ 140 mm height
Vibrating frequency, f	8, 16, 24, 32 Hz
Vibrating amplitude, A	1.09, 1.94, 4.37, 17.48 mm
Simulation time step, Δt	10^{-7} s

with the vibrating base replaced by particles undergoing a similar type of imposed oscillatory motion to represent a "bumpy" vibrating base. In the second part of this study, the "grain size" of this bumpy base was varied in the range of 0.1–2.0 mm to investigate its effect on the collective behavior of the vibrated granular bed.

III. RESULTS AND DISCUSSION

Figure 1(a) shows a snapshot of the simulated vibrated granular bed system obtained in the present study, operating under the conditions $f=16$ Hz and $A=4.37$ mm ($\Gamma=4.50$) corresponding exactly to those used by Deng and Wang [8] in their experiments. It may be seen that the standing-wave pattern as observed physically by the previous authors have been reproduced computationally. More importantly, it may also be observed that a layer of granular materials of one-particle thickness is adhered to the vibrating base when the latter is at the lowest position of its oscillatory motion. In this regard, there is a close resemblance between this simulation result and the experimental observation made by the previous authors (Fig. 2 of [8]). With reference to the postulate made earlier, the fairly low ε_b value applied in the present simulation has resulted in moderately inelastic particle-base collisions, leading to particles remaining in close proximity to the base after collisions and the formation of the observed thin granular layer. Energy imparted by the vibrating base to the first layer of granular materials is quickly dissipated by inelastic particle-base collisions, resulting in the formation of a monolayer next to the base. However, occasional collisions between particles in this monolayer and those from the bulk may be sufficiently energetic to knock the former away from the base, giving rise to the discontinuous appearance of the monolayer as seen in Fig. 1(a). Although this monolayer of granular materials may undergo short periods of free fall and deformation during the downward acceleration phase of the vibrating base, the configuration of it being almost parallel to the base is reestablished quickly upon collisions between particles in this layer with the base. Figure 1(b) shows a snapshot of the same vibrated granular bed system with the vibrating base in contact with the granular materials. It may be imagined that the

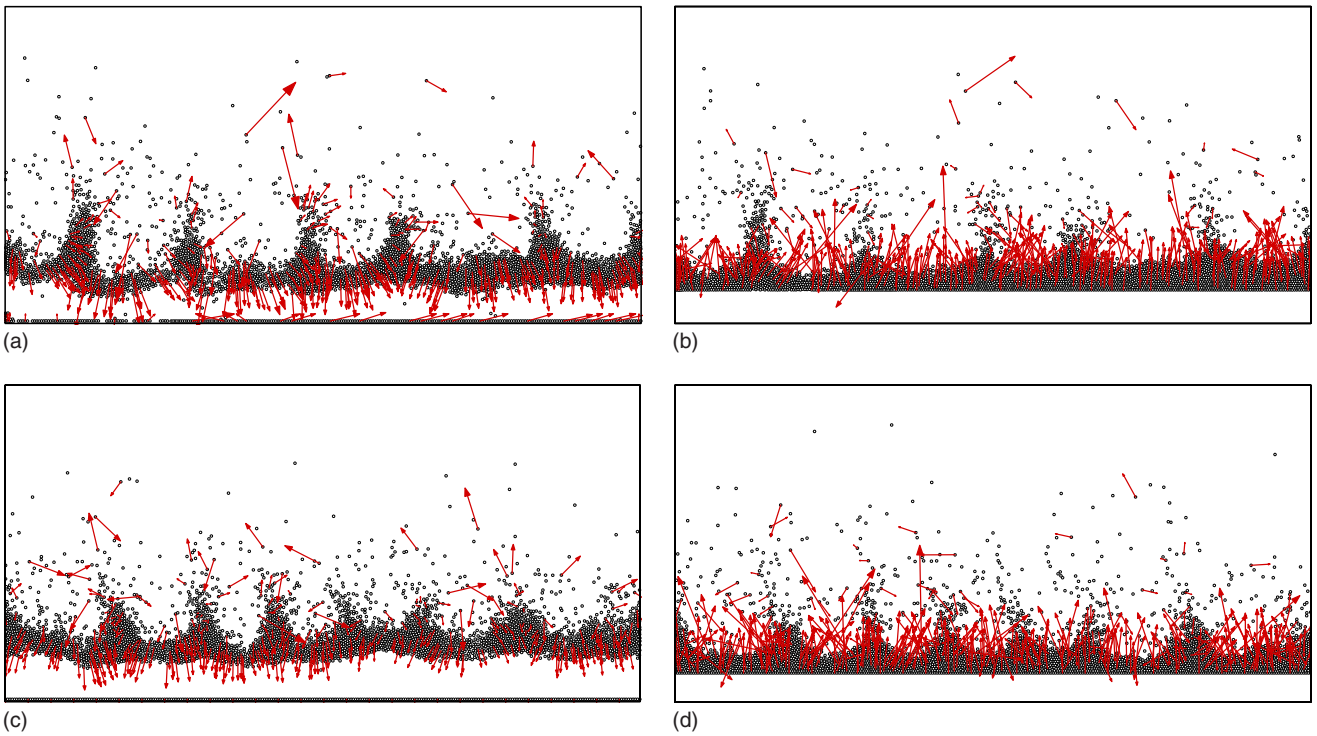

FIG. 1. (Color online) Standing-wave pattern formation in vibrated granular beds operating under the conditions $f=16$ Hz and $A=4.37$ mm ($\Gamma=4.50$) with (a) flat base at approximately its lowest position in the oscillation cycle, (b) flat base in contact with the granular bed, (c) bumpy base at approximately its lowest position, and (d) bumpy base in contact with the granular bed. Velocity vectors show instantaneous directions of motion of selected solid particles.

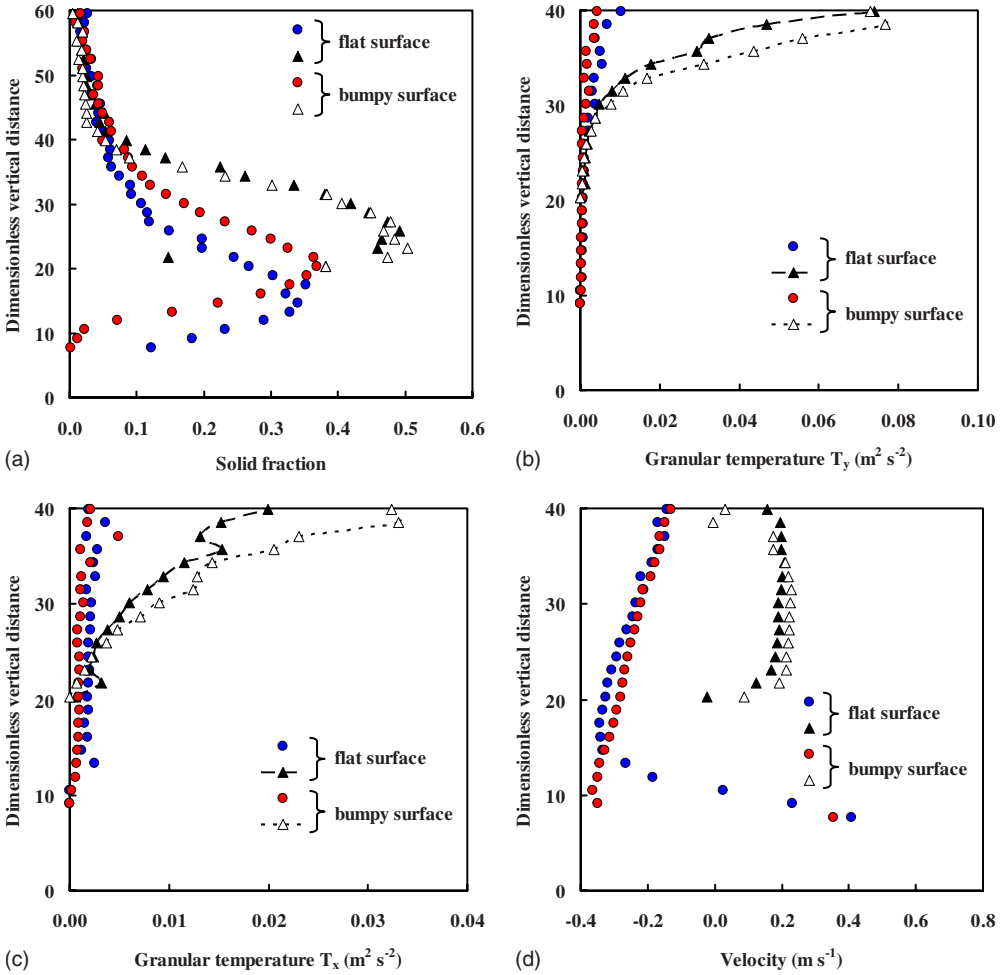

FIG. 2. (Color online) Spatially averaged (a) solid fraction, (b) granular temperature T_y, (c) granular temperature T_x, and (d) solid velocity profiles for vibrated granular beds with flat and bumpy bases operating under the conditions $f=16$ Hz and $A=4.37$ mm ($\Gamma=4.50$). Profiles denoted by circular symbols correspond to the phase of oscillation of the granular bed where the base is at its lowest position while those denoted by triangular symbols correspond to the phase where the base is in contact with the granular bed. Vertical distances have been nondimensionalized by particle diameter.

vibrating base has elevated the thin granular layer to come into contact with the granular bed. As such, particle-base collisions in each cycle of the oscillatory motion of the base are then between the bulk granular materials and the thin granular layer adhered to the base effectively. In other words, a fairly low value of the coefficient of restitution for particle-base collisions has resulted, in effect, in the "formation" of a bumpy vibrating base due to the adhesion of a thin granular layer to the surface of the base. It is then natural to explore whether an artificially imposed bumpy vibrating base would also give rise to the same standing-wave pattern observed. To this end, we replace the vibrating base with a row of 0.5 mm glass beads with the same material properties as those used in the granular bed. A total of 280 glass beads are used to form the bumpy base while the total number of particles in the bulk is maintained at 4000. The same sinusoidal motion is imposed on this row of glass beads to simulate a vibrating base with a bumpy surface. Figures 1(c) and 1(d) show snapshots of the system in the same phases as those shown in the earlier two panels, respectively. The qualitative structure of the standing-wave pattern in terms of the number of wave crests and their relative positions within the system are very similar between the two sets of simulations. The velocity vectors depicting the directions of motion of particles at the two-time instants are also comparable for the two cases.

Figure 2(a) shows a quantitative comparison of the spatially averaged solid fraction profiles between the vibrated granular beds with flat and bumpy bases. Profiles denoted by circular symbols correspond to the phase of vibration of the granular bed where the base is at its lowest position while those denoted by triangular symbols correspond to the phase where the base is in contact with the granular bed, instances of which have been shown in Figs. 1(a) and 1(c) and Figs. 1(b) and 1(d), respectively. It may be observed that there are significant variations in solid fraction profiles for the vibrated granular beds at different phases of their oscillation cycles. However, the discrepancies in these profiles between beds with flat and bumpy surfaces, and those corresponding to intermediate phases of oscillation which have not been shown here for the sake of brevity, are much less significant. All profiles in Fig. 2(a) exhibit maximum points in solid fraction values which are typical of the standing-wave pat-

tern in vibrated granular bed systems. Interestingly, profiles corresponding to the phase where the base is at its lowest position seem to be displaced from each other by a vertical translation. This may imply that the entire bulk of granular materials in the vibrated bed with a bumpy base have been elevated to a slightly higher position but with its overall granular pattern and solid distribution within the bulk being quantitatively similar to its counterpart in the vibrated bed with a flat base. Figures 2(b)–2(d) show that granular temperature and solid velocity profiles for the two types of vibrated granular bed systems are also quantitatively similar. Here, the two components of granular temperature are defined as $T_y=\frac{1}{2n}\Sigma_{i=1}^{n}(v_{y,i}-\overline{v_y})^2$ and $T_x=\frac{1}{2n}\Sigma_{i=1}^{n}(v_{x,i}-\overline{v_x})^2$, respectively, where $v_{y,i}$ and $v_{x,i}$ are the vertical and horizontal components of velocity of the ith particle, and $\overline{v_y}$ and $\overline{v_x}$ are the corresponding mean velocities. For the highly vibrated granular bed systems considered in this study, Figs. 2(b) and 2(c) show that granular temperatures are strongly anisotropic, especially for the phase of oscillation where the base is in contact with the granular bed. For both types of granular bed systems, vertical components of granular temperature are generally double in magnitude of their horizontal counterparts. Nevertheless, a close similarity is maintained for granular temperature profiles between the two types of granular systems at the same phase of oscillation. Figure 2(d) shows that the solid velocity profiles also exhibit such a characteristic. This is the numerical evidence showing the equivalence, both qualitatively as well as quantitatively, of vibrated granular bed systems with flat inelastic bases and those with bumpy relatively more elastic bases (where elasticities here refer to those associated with particle-base collisions). This observation may have important implications for future theoretical development of more sophisticated continuum models of such vibrated granular bed systems, in particular, with regards to the way the vibrating base is defined as a boundary condition. As can be imagined, it is difficult in principle to provide a realistic description of the vibrating base condition in a continuum model of the system. In a recent linear stability analysis study, Deng and Wang [19] defined the vibrating base of their vibrated bed system to be a source of pseudothermal energy. The nature of the vibrating base, such as with regards to the elasticities of particle-base collisions, cannot be taken into account directly with this form of definition for the vibrating base boundary condition. The present study shows that, in the case of a vibrated granular bed with an inelastic base, the equivalent of a "boundary layer" of solid particles with physical properties similar to those in the bulk is expected to form on the surface of the vibrating base. The solid fraction on the vibrating base is also expected to be equivalent to that for a monolayer of solid particles adhered to the base. These proposed definitions of boundary conditions may provide more realistic descriptions of vibrated granular bed systems with inelastic vibrating bases using continuum models.

As shown in Table I earlier, the above numerical experiment was carried out for four different values of both the vibrating frequency and amplitude, giving a total of 16 simulations and Γ values in the range of 0.28–72.0. In all these cases, a similar conclusion as that obtained for the previous one presented may be reached, that is, a vibrated granular bed with an inelastic (coefficient of restitution of 0.46) flat base is equivalent, both qualitatively and quantitatively, to one with a more elastic (coefficient of restitution of 0.86) but bumpy base. For sake of brevity, we select one other case which exhibits a different regime from the standing waves seen earlier to substantiate this conclusion. Figure 3(a) shows that under the conditions $f=32$ Hz and $A=4.37$ mm ($\Gamma=18.0$), a vibrated granular bed with a flat base exhibits what is commonly referred to in the literature as the arching phenomenon. As with the previous case, a monolayer of solid particles is also seen here adhered to the vibrating base due to the inelasticity of particle-base collisions. Figure 3(b) shows the vibrated granular bed with a bumpy base operating under the same conditions and forming the same type of granular arches. The corresponding velocity vectors of the granular solids (data not shown for brevity) are also remarkably similar for the two types of vibrated granular bed systems. Quantitatively, it may also be observed from Figs. 4(a)–4(d) that the spatially averaged solid fraction, granular temperature, and solid velocity profiles, respectively, corresponding to the phase of oscillation shown in the previous figure for the two types of vibrated granular beds, are also very similar. Solid fraction profiles for both systems exhibit maximum values of about 0.3 at a vertical position of about 30 particle diameters from the base. As with the standing-wave pattern considered earlier, granular temperatures are highly anisotropic with vertical components approximately twice that of the corresponding horizontal components. Solid velocity profiles for the two types of vibrated granular beds show a close correspondence and are fairly linear in the 40–60 particle diameter section considered. Figures 5(a) and

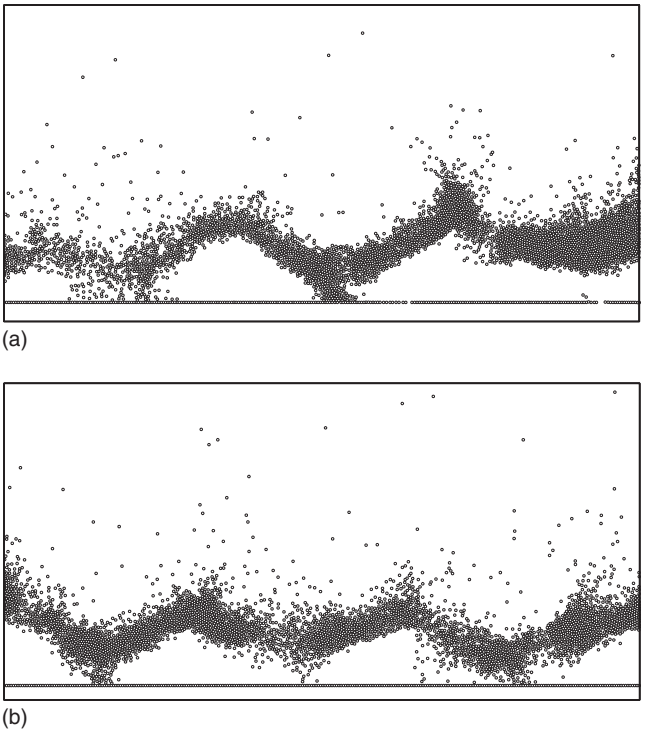

FIG. 3. Arching phenomenon in vibrated granular beds with (a) flat and (b) bumpy bases operating under the conditions $f=32$ Hz and $A=4.37$ mm ($\Gamma=18.0$).

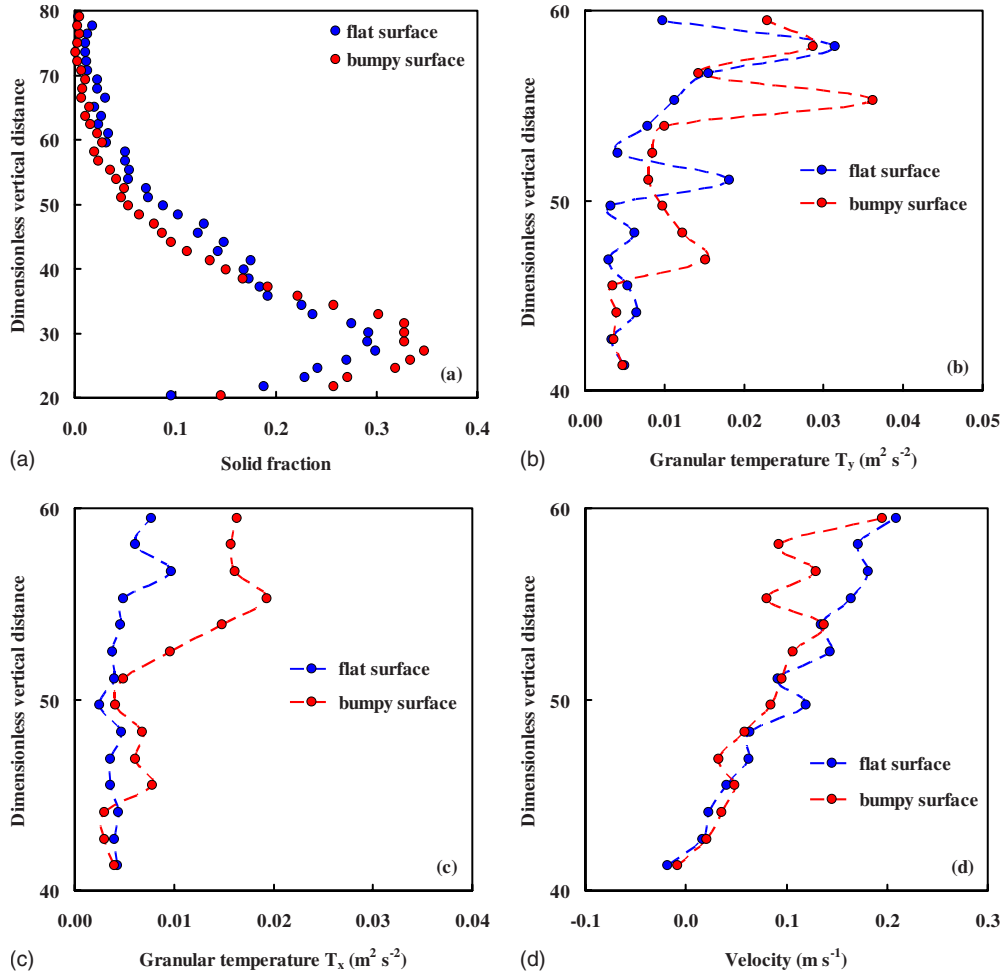

FIG. 4. (Color online) Spatially averaged (a) solid fraction, (b) granular temperature T_y, (c) granular temperature T_x, and (d) solid velocity profiles for vibrated granular beds with flat and bumpy bases operating under the conditions $f=32$ Hz and $A=4.37$ mm ($\Gamma=18.0$). The phase of oscillation corresponds to that shown in the previous figure for the two types of vibrated granular beds. Vertical distances have been nondimensionalized by particle diameter.

5(b) show the formation of "tall" standing waves in vibrated granular beds with flat and bumpy bases, respectively, when the operating conditions are $f=8$ Hz and $A=17.48$ mm ($\Gamma=4.50$). The structure of these standing waves, with regards to their heights, widths, and wavelengths within the two types of beds, are again seen to be very comparable. More quantitatively, the instantaneous snapshots of the tall standing-wave structures show that $h_1 \approx h_2 \approx 125d$ and $w_1 \approx w_2 \approx 112d$. It may be mentioned at this point that, although not presented in this paper for sake of brevity, such similarities in the collective behaviors of vibrated granular bed systems with flat and bumpy bases and their corresponding solid fraction, granular temperature, and solid velocity profiles have also been observed for the other operating conditions listed in Table I investigated in this study.

With these observations, it was deemed prudent to then investigate the effects of grain size of a bumpy base on the collective behavior of a vibrated granular bed. To this end, we repeated the bumpy base simulations using particles of diameters 0.1, 1.0, and 2.0 mm as the base while keeping the size, number, and material properties of particles in the bulk unchanged. The numbers of particles used to form the bumpy base are 1400, 140, and 70, respectively, while the total number of particles in the bulk is maintained at 4000. Figures 6(a)–6(c) show snapshots of vibrated granular bed systems with the three types of bumpy bases, respectively. The operating conditions applied were $f=16$ Hz and $A=4.37$ mm ($\Gamma=4.50$), and it may be noted that the corresponding snapshot for the case where the grain size of the bumpy base is equal to the particle size of the bulk granular materials has been presented previously in Fig. 1(c). Standing waves of similar amplitudes and wavelengths are formed in all these cases with seemingly little dependence on bumpiness of the vibrating base. Figures 7(a)–7(d) show that there are no significant differences in the spatially averaged solid fraction, granular temperature, and solid velocity profiles for the vibrated granular beds with the four types of vibrating bases. The same phenomenon has been observed for the other operating conditions investigated in this study. The solid fraction profiles for the various systems with different grain sizes of the bumpy base collapse almost perfectly onto one another and with all profiles exhibiting a maximum point at a vertical position of about 20 particle diameters from the base. Interestingly, profiles for the two components of granular tem-

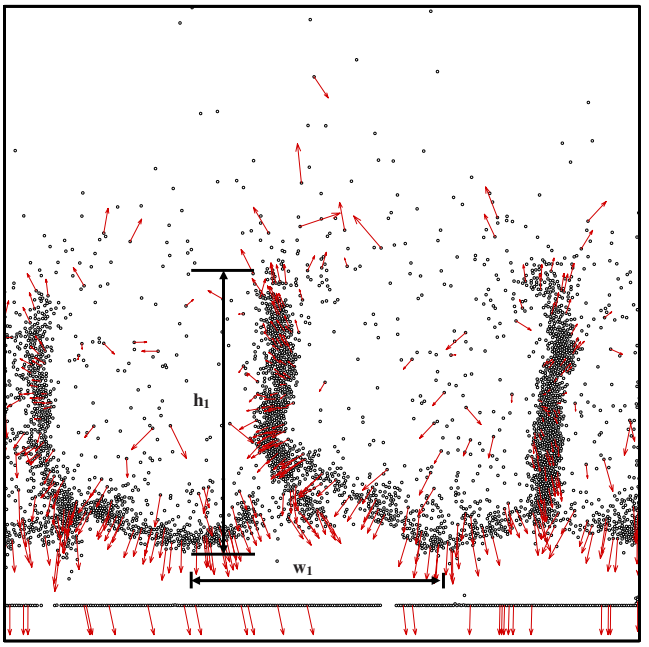

(a)

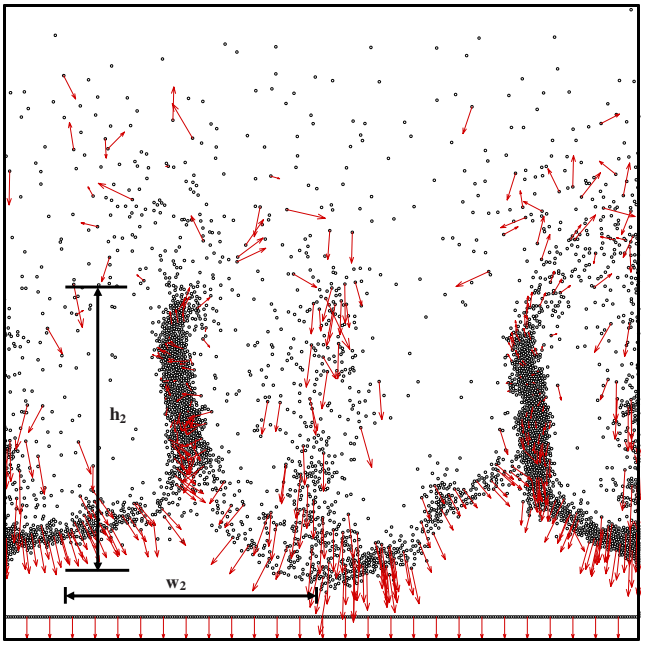

(b)

FIG. 5. (Color online) Tall standing waves in vibrated granular beds with (a) flat and (b) bumpy bases operating under the conditions $f=8$ Hz and $A=17.48$ mm ($\Gamma=4.50$). The instantaneous snapshots show that $h_1 \approx h_2 \approx 125d$ and $w_1 \approx w_2 \approx 112d$. Velocity vectors show instantaneous directions of motion of selected solid particles.

perature seem to imply that granular temperature is less anisotropic for the phase of oscillation where the base is approximately at the lowest position, regardless of grain sizes of the bumpy base. This is consistent with the observation made earlier where anisotropy in granular temperature occurs when the vibrating base is in contact with the granular bed. Figure 7(d) shows that solid velocity profiles for the

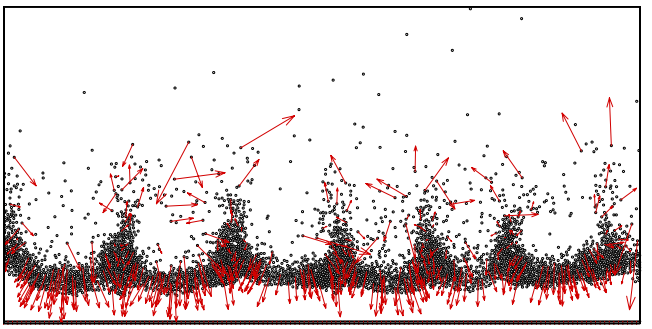

(a)

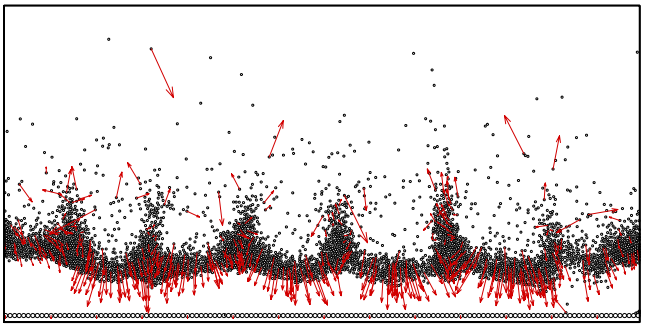

(b)

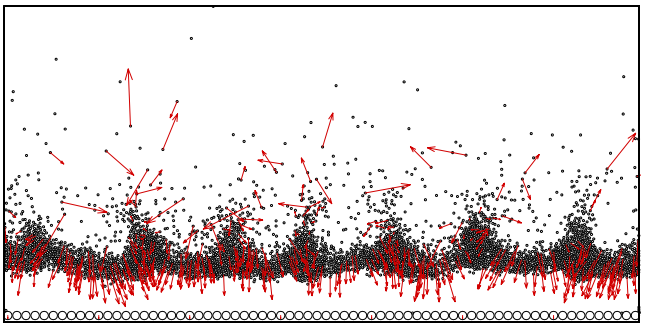

(c)

FIG. 6. (Color online) Standing-wave pattern formation in vibrated granular beds operating under the operating conditions $f=16$ Hz and $A=4.37$ mm ($\Gamma=4.50$) with particles of diameters (a) 0.1, (b) 1.0, and (c) 2.0 mm as the bumpy base. The corresponding snapshot for the case where the grain size of the bumpy base is equal to the particle size of the bulk granular materials has been presented previously in Fig. 1(c).

four types of systems show good quantitative agreement and are highly linear for the phase of oscillation considered. Based on these observations, it would be reasonable to suggest that effects of different grain sizes of a bumpy vibrating base are negligible for the range of operating conditions considered here. We present a final illustration using simulation results obtained with $f=32$ Hz and $A=1.09$ mm ($\Gamma=4.50$). The typical granular behavior observed under this set of operating conditions is heap formation and qualitatively similar granular distributions are obtained regardless of the grain size imposed on the base. Quantitatively, the solid fraction, granular temperature, and solid velocity profiles, as presented in Figs. 8(a)–8(d), respectively, are also similar for the vibrated granular bed systems with the four types of bases. The solid fraction profiles show good quantitative

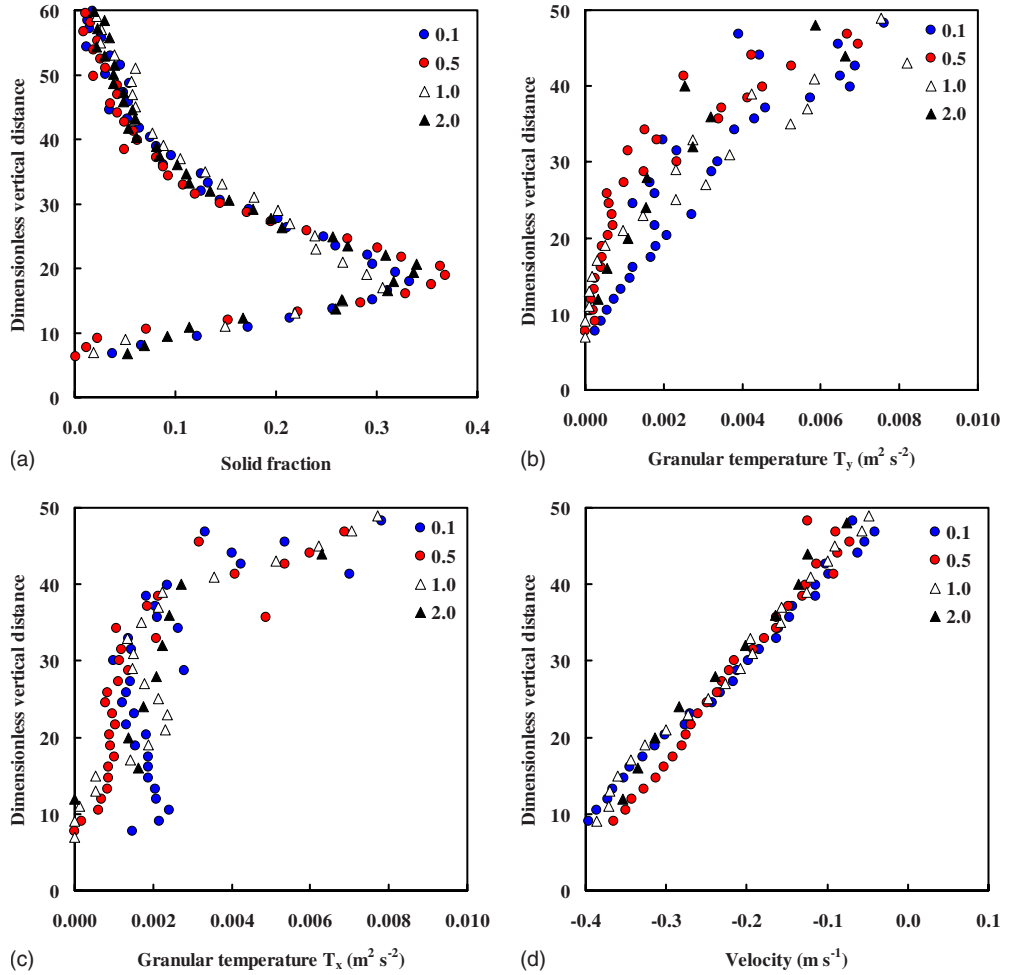

FIG. 7. (Color online) Spatially averaged (a) solid fraction, (b) granular temperature T_y, (c) granular temperature T_x, and (d) solid velocity profiles for vibrated granular beds with particles of diameters 0.1, 0.5, 1.0, and 2.0 mm as the bumpy base operating under the conditions $f=16$ Hz and $A=4.37$ mm ($\Gamma=4.50$). Vertical distances have been nondimensionalized by particle diameter.

agreement between the different types of bumpy bases while granular temperature and solid velocity profiles show only good qualitative agreement. The profiles presented here correspond to the phase of vibration where the base is in contact with the granular bed. As such, the slight quantitative differences may imply a small but discernible effect of the bumpiness of the vibrating base.

It is appropriate at this point to mention a more recent work reported by Carrillo *et al.* [20] in which standing-wave patterns in a vibrated granular bed were reproduced computationally in quantitative agreement using both event-driven molecular-dynamics and hydrodynamic simulations based on continuum models. However, despite close similarities in simulation results obtained from the two different numerical approaches in terms of velocity fields, granular temperatures, and convection patterns, it was observed that granular materials in the hydrodynamic simulations were always in contact with the vibrating base while a gap formed when the base moved downward in the molecular-dynamics simulations, giving rise to zero solid fraction just above the vibrating base. The authors attributed this difference to the manner in which the boundary condition was defined for the vibrating base (as an impenetrable adiabatic surface) and the relatively low coefficient of restitution specified for the base. On the other hand, they explained the good agreement between the two different numerical approaches as due to the fact that the dynamics involved was mostly Eulerian in nature, and other details such as constitutive relations and transport coefficients were of secondary importance. Here, we would like to further suggest based on results of the present study that the absence of a gap between the bulk granular materials and the vibrating base in their hydrodynamic simulations, hence effectively leading to the formation of a bumpy base, is not expected to cause a significant difference in bulk granular behavior from a vibrated granular bed system whose bumpiness of the base is zero, or essentially flat.

It has been well established in the research literature that the behaviors of vibrated granular bed systems are strongly dependent on a few important properties that characterize the system, such as the ratio of system to particle size, thickness of the granular bed defined by the number of layers of granular materials within the system at rest, etc. The result of the present study seems to imply that bumpiness of the vibrating base does not represent a characteristic property that will influence the behavior of the system significantly. Here, we will attempt to propose an explanation for this somewhat

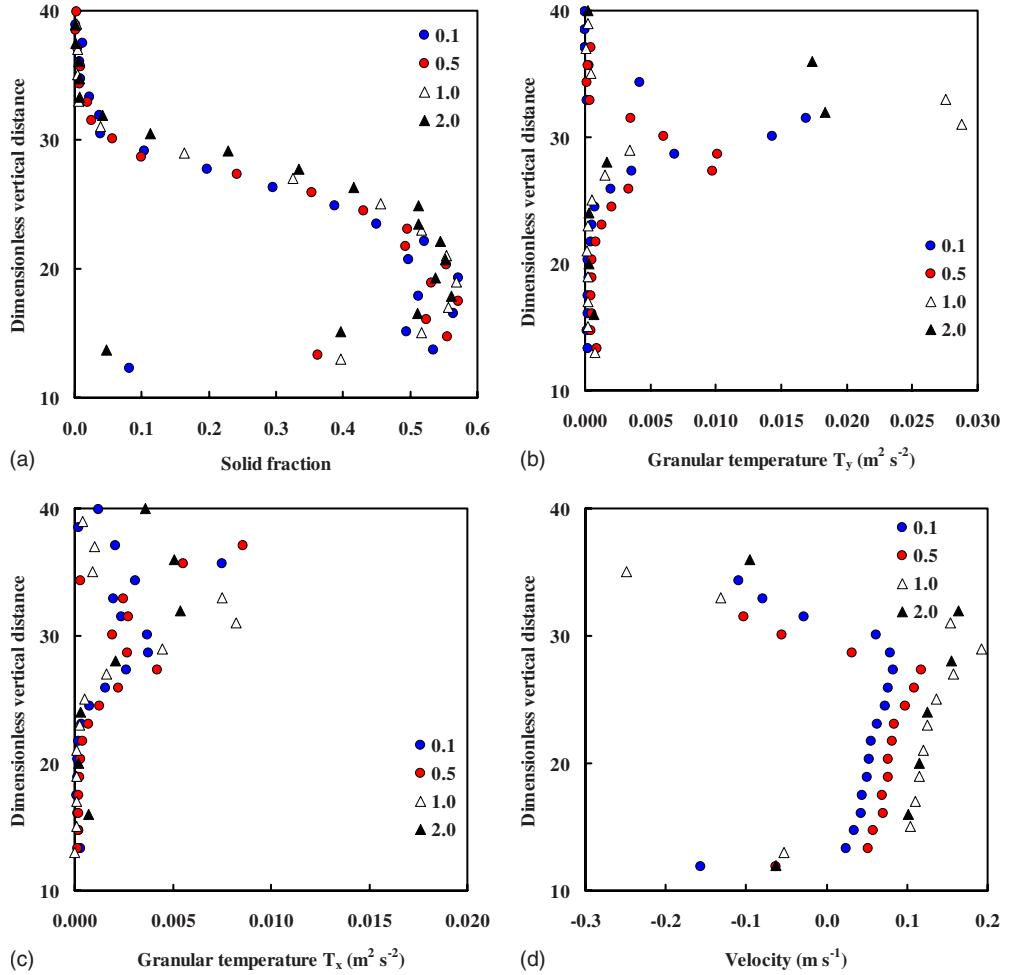

FIG. 8. (Color online) Spatially averaged (a) solid fraction, (b) granular temperature T_y, (c) granular temperature T_x, and (d) solid velocity profiles for vibrated granular beds with particles of diameters 0.1, 0.5, 1.0, and 2.0 mm as the bumpy base operating under the conditions $f=32$ Hz and $A=1.09$ mm ($\Gamma=4.50$). Vertical distances have been nondimensionalized by particle diameter.

counterintuitive observation. In a vibrated granular bed system, the vibrating base represents a source of energy for the bulk granular materials. Energy is inputted through the vibrating base and dissipated through inelastic particle-particle or particle-wall collisions. The flux of energy or granular temperature, which can be characterized by the dimensionless parameter Γ, has a strong influence on the behavior and type of pattern formed by the granular materials. Imperfections or bumpiness in the vibrating base surface may have the effect of introducing additional localized perturbations to the positions and velocities of particles which come into direct contact with the base. However, in principle, the mean flux of granular temperature provided by a bumpy base should not differ from its flat counterpart operating at the same value of Γ. This is supported by the almost identical values of granular temperature as well as slopes of the granular temperature curves between systems with flat and bumpy bases near the position of the base, as seen in all such figures presented in this paper. We further argue that, within the range of operating conditions and bumpiness of the vibrating base investigated in this study, localized perturbations caused by a bumpy base are quickly nullified or damped out via inelastic collisions between the affected particles and those in the rest of the bulk. Such perturbations are neither sufficiently amplified nor propagated through the bulk to the extent of altering the behavior of the system. It may certainly be envisaged that a very bumpy or sufficiently "deformed" base will almost definitely result in significant differences in relative positions between large portions of the bulk granular materials, even in the rest state. A detailed investigation of this aspect of vibrated granular bed systems may constitute the subject of a future research study.

IV. CONCLUSIONS

We have demonstrated through numerical simulations the equivalence of vibrated granular bed systems with flat inelastic bases and bumpy relatively more elastic bases. Here, elasticity refers to that associated with collisions between solid particles in the granular bulk and the vibrating base. In vibrated granular bed systems with flat inelastic bases, a monolayer of granular materials was observed to form dynamically on the surface of the base due to inelastic collisions such that vibration of the bulk granular materials occurred effectively on a bumpy oscillating surface. Within the range of operating conditions investigated in this paper as defined

by the vibrating frequency and amplitude or, equivalently, the dimensionless acceleration parameter, the collective granular behavior, solid fraction, granular temperature, and solid velocity profiles were found to be similar for systems with flat inelastic or bumpy and more elastic bases. The bumpiness of bumpy bases, as defined by the grain size of particles constituting the base, was also observed to have insignificant effects on the qualitative behavior as well as the various quantitative profiles of the vibrated granular bed systems. These interesting but somewhat counterintuitive properties of vibrated granular bed systems do not seem to have been reported in the research literature to date. However, it should also be noted that the number of numerical experiments carried out in this study is limited and a large portion of the parameter space remains unexplored at this stage. Therefore, the conclusions made in this paper should not be generalized as universal properties of vibrated granular bed systems and we leave investigations of limits at which such similarities between systems with the two types of bases collapse to future studies. It would also be important to corroborate the numerical simulation results reported here with physical experimentation and to extend the current work to three-dimensional systems to verify that the phenomena observed here are not simply artifacts of the two dimensionality of the vibrated granular bed systems investigated in this study.

ACKNOWLEDGMENT

This study has been supported by the National University of Singapore under Grant No. R-279-000-275-112.

[1] H. K. Pak and R. P. Behringer, Phys. Rev. Lett. **71**, 1832 (1993).
[2] F. Melo, P. B. Umbanhowar, and H. L. Swinney, Phys. Rev. Lett. **72**, 172 (1994).
[3] F. Melo, P. B. Umbanhowar, and H. L. Swinney, Phys. Rev. Lett. **75**, 3838 (1995).
[4] P. B. Umbanhowar, F. Melo, and H. L. Swinney, Nature (London) **382**, 793 (1996).
[5] L. S. Tsimring and I. S. Aranson, Phys. Rev. Lett. **79**, 213 (1997).
[6] K. M. Aoki and T. Akiyama, Phys. Rev. Lett. **77**, 4166 (1996).
[7] C. Bizon, M. D. Shattuck, J. B. Swift, W. D. McCormick, and H. L. Swinney, Phys. Rev. Lett. **80**, 57 (1998).
[8] R. Deng and C. H. Wang, Phys. Fluids **15**, 3718 (2003).
[9] Y. Lan and A. D. Rosato, Phys. Fluids **7**, 1818 (1995).
[10] A. B. Yu, X. Z. An, R. P. Zou, R. Y. Yang, and K. Kendall, Phys. Rev. Lett. **97**, 265501 (2006).
[11] S. L. Conway and B. J. Glasser, Phys. Fluids **16**, 509 (2004).
[12] E. W. C. Lim, C. H. Wang, and A. B. Yu, AIChE J. **52**, 496 (2006).
[13] E. W. C. Lim, Y. Zhang, and C. H. Wang, Chem. Eng. Sci. **61**, 7889 (2006).
[14] E. W. C. Lim and C. H. Wang, Ind. Eng. Chem. Res. **45**, 2077 (2006).
[15] E. W. C. Lim, Y. S. Wong, and C. H. Wang, Ind. Eng. Chem. Res. **46**, 1375 (2007).
[16] E. W. C. Lim, Chem. Eng. Sci. **62**, 4529 (2007).
[17] H. P. Zhu, Z. Y. Zhou, R. Y. Yang, and A. B. Yu, Chem. Eng. Sci. **63**, 5728 (2008).
[18] E. W. C. Lim, Ind. Eng. Chem. Res. **47**, 481 (2008).
[19] R. Deng and C. H. Wang, J. Fluid Mech. **492**, 381 (2003).
[20] J. A. Carrillo, T. Poschel, and C. Saluena, J. Fluid Mech. **597**, 119 (2008).